Jinst

Published by IOP Publishing for Sissa Medialab

Received: *January 18, 2020*
Revised: *February 18, 2020*
Accepted: *March 3, 2020*
Published: *April 6, 2020*

Detection and discrimination of α- and β-radiation with plastic scintillators based on pulse shape discrimination

Z.H. Zhang,[a,b,d] **Y.F. Zhang,**[c] **C.Y. Hu,**[b] **S. Feng,**[b] **J.J. Zhu,**[b] **B. Liao,**[a,d,1] **D.K. Liu,**[b,e] **Q. Zhou**[a] **and H.R. Wang**[a]

[a] *Key Laboratory of Beam Technology of Ministry of Education, College of Nuclear Science and Technology, Beijing Normal University, Beijing, 100875, China*
[b] *School of Nuclear Science and Technology, University of South China, Hengyang, 421001, China*
[c] *Institute of High Energy Physics, Chinese Academy of Sciences, Beijing, 100049, China*
[d] *Beijing Radiation Center, Beijing, 100875, China*
[e] *Xi'an Nuclear Instrument Factory, Xi'an, 710061, China*

E-mail: liaobingz@bnu.edu.cn

Abstract: There is a need for more convenient and effective methods for detecting and discriminating between α- and β-radiation. In this work, two plastic scintillator detectors were used to detect and discriminate between α- and β-radiation based on digital pulse shape discrimination (PSD). The charge comparison method (CCM) performed better than the time comparison method (TCM), and Detector A (with ZnS doping) showed better results than those of Detector B (without ZnS doping). With Detector A, the total rate of misidentification was approximately 0.25% with the appropriate discrimination parameters; with Detector B, the total rate of misidentification was approximately 1.5%. Both detectors showed improved discrimination compared with most commercial detectors. This method is a promising means for improving the effectiveness of the detection and discrimination of α- and β-radiation based on PSD.

Keywords: Digital signal processing (DSP); Particle identification methods; Radiation monitoring; Ion identification systems

[1] Corresponding author.

https://doi.org/10.1088/1748-0221/15/04/P04008

2020 JINST 15 P04008

Contents

2020 JINST 15 P04008

1 Introduction

There are many differences between α- and β-radiation. One of the most obvious differences is that their radiation quality factors have distinct radiological protection. β-radiation has a quality factor of 1, and α-radiation has a quality factor of 20.

α- and β-radiation can be discriminated by their energy spectra. However, sample surface contamination impacts radiation particle detection, leading to energy losses. The α-particle rapidly loses energy in the air gap prior to reaching the detector window, which results in a large lower energy spectrum spread, overlapping with that of β-radiation.

To address these issues, plastic scintillators are doped with zinc sulfide (ZnS). ZnS has a large fluorescent yield for α-radiation but not β-radiation. With ZnS, α-radiation events are distributed to higher energy sections of the energy spectrum, whereas β-radiation events are distributed in lower energy sections. Using ZnS, when products are tested using a clean radiation source, α- and β-radiation can then be discriminated by their energy spectra. However, in sampling dirty sources, some α-radiation are misidentified as β-radiation.

There is a need to detect and discriminate α- and β-radiation using convenient and more effective methods. Pulse shape discrimination (PSD), the charge comparison method (CCM) and the time comparison method (TCM) are commonly used in the discrimination of neutron- and γ-radiation [1–6]. I. Kreslo et al. reported on PSD with a liquid scintillator [7]. H. Bagán et al. used a plastic scintillator to discriminate α- and β-radiation; the rates of misidentification were lower than 7% [8]. However, the effectiveness of PSD methods remains unknown.

In recent years, PSD techniques have been used in the discrimination of α- and γ-radiation [9, 10]. In this work, the detection and discrimination of α- and β-radiation were

attempted with plastic scintillators based on PSD. To evaluate the effectiveness of digital PSD, two methods were tested using a special scintillator (with ZnS doping) and a non-special scintillator (without ZnS doping) for discriminating between α- and β-radiation.

2 Pulse shape discrimination

2.1 Differences in nuclear pulse shapes

Electrons are light compared with α-particles. The energy loss per collision of an electron is greater than that of an α-particle when interacting with matter. Thus, their energy-loss rates (dE/dx) are different as indicated by different luminescence rates measured by scintillators; this results in differences in the output current of photomultiplier tubes (PMTs). The resultant different nuclear pulse shapes from a detector can be approximately described by Formula (2.1). The nuclear pulse shapes of α- and β-radiation have different fast and slow components [11, 12].

$$v(t) = v_s \cdot e^{-t/\tau_s} + v_f \cdot e^{-t/\tau_f} \tag{2.1}$$

where v_s is the voltage of the slow component, v_f is the voltage of the fast component, τ_s is the slow time constant, and τ_f is the fast time constant.

2.2 Charge comparison method

An analogue circuit is used to implement the CCM through current integration by capacitance and the associated ballistic deficit. In digital signal processing, integration in the CCM is replaced by a summation: $\sum_{i=k}^{m} v_i$. As Formula (2.2) shows, to eliminate the influence of different energy depositions on the same kind of particle, the summation $\sum_{i=k}^{m} v_i$ (corresponding to the short window) is normalized by the summation $\sum_{i=0}^{n} v_i$ of "total charge-quantity" (corresponding to the long window). The short window is shown in figure 1; the horizontal axis, which presents the sampling serial number (i), gives the time information of each digitized waveform (i.e. 1 ns interval for 1 GHz sampling rate digitizer). The long window includes the whole pulse shape.

$$P_{CCM} = \sum_{i=k}^{m} v_i / \sum_{i=0}^{n} v_i \tag{2.2}$$

where n is the number of the last sampling point of a complete digital discrete nuclear pulse (starting at 0), k is the starting number of the short window, and m is the ending number of the short window.

2.3 Time comparison method

The TCM determines the voltage signal by integrating over the current measurements. When measuring a unipolar nuclear pulse, CR differentiation is used to convert to a bipolar pulse. Then, the duration between the leading edge and crossing zero is determined. The zero-crossing point of the bipolar nuclear pulse corresponds to the peak point of the unipolar nuclear pulse; this is also referenced as the "rising time method". The digital TCM directly processes unipolar nuclear pulse signals. The definition of the rising time of the unipolar pulse is shown in figure 1.

2020 JINST 15 P04008

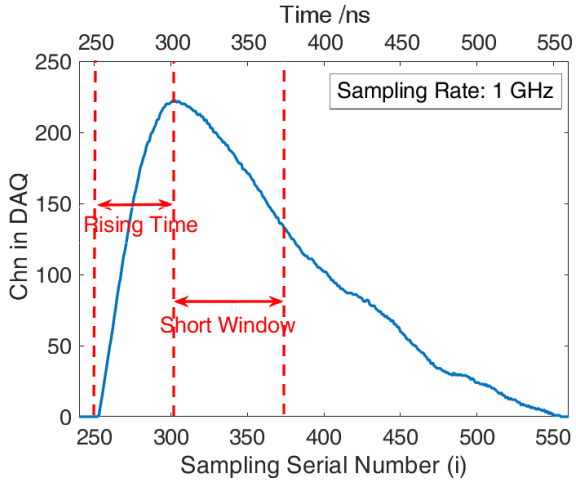

Figure 1. Diagram of discrimination parameters.

3 Experiment

3.1 Experimental setup

Two plastic scintillator detectors were used. One detector ("Detector A") was produced by Beijing Gaonengkedi Science and Technology Co., Ltd., and was equally doped with ZnS and para-terphenyl to detect α- and β-radiation. As shown in figure 2(a), the scintillator had a 5-cm diameter and a 1-mm thickness. The scintillator was coupled to a PMT (Hamamatsu CR105-03) using a 1-cm-thick optical guide and silicone oil. The other detector ("Detector B") was produced by Beijing Hoton Nuclear Technology Co., Ltd, and was only doped with para-terphenyl (figure 2(b)).

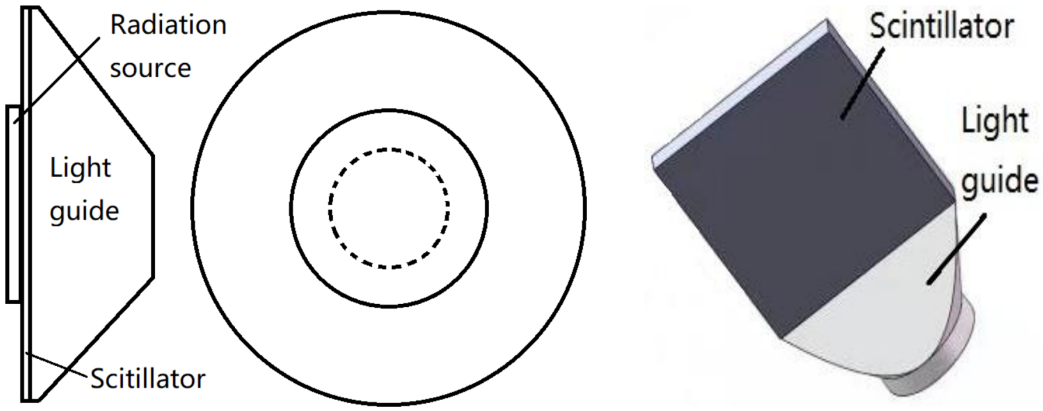

(a) Plastic scintillator A.

(b) Plastic scintillator B.

(c) The schematic diagram of the experimental setup.

Figure 2. The detectors and the experimental setup.

2020 JINST 15 P04008

The experimental setup is shown in figure 2(c). A plastic scintillator and a PMT constituted a plastic scintillator detector. The PMT was powered by a high voltage −800 V DC supply (Ortec 556H). The capacitance of a preamplifier (Ortec 113) was 100 pF. A main amplifier (Ortec 474) was used to reverse and linearly amplify the nuclear pulse from the preamplifier to the appropriate amplitude for data acquisition. Nuclear pulses were collected by data acquisition (Caen DT5751) at a sampling rate of 1 GHz and sent to a computer. The α-radiation source was ^{241}Am, and the β-radiation source was ^{90}Sr. The nuclear pulses of α- and β-particles were randomly selected and peak-normalized as shown in figure 3.

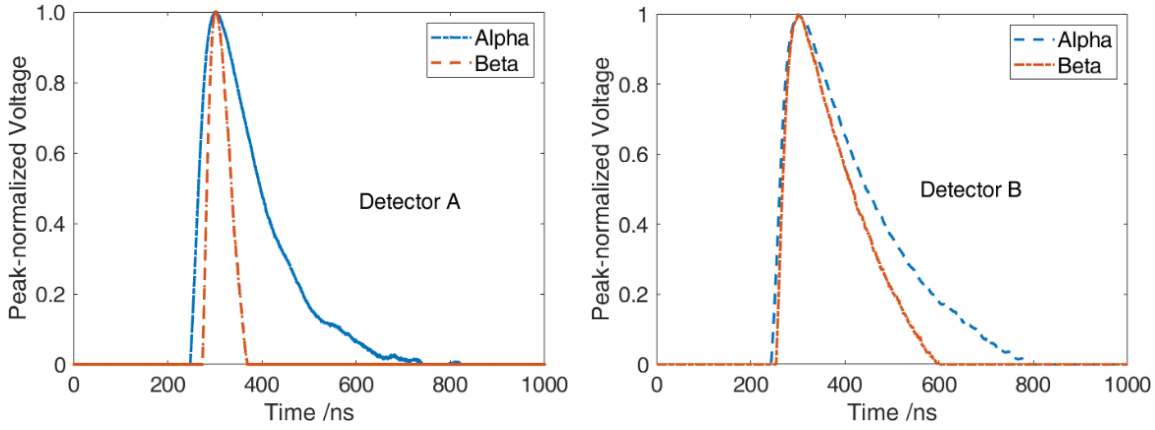

Figure 3. Nuclear pulse shapes of α- and β-particle.

3.2 Determination of the short window

After discrimination, the distributions of α- and β-radiation were approximately two Gaussian distributions. In the discrimination of neutron- and γ-radiation, figure of merit (FoM) values for the PSD methods can be calculated by Formula (3.1) [13–15]:

$$\mathrm{FoM} = \left|\left(\mu_{\mathrm{n}} - \mu_{\gamma}\right) / \left(\mathrm{FWHM}_{\mathrm{n}} + \mathrm{FWHM}_{\gamma}\right)\right| \tag{3.1}$$

where μ is the mean value of the Gaussian distribution, FWHM is the full width at half maximum of the Gaussian distribution, and the subscript indicates the corresponding radiation.

Ten thousand pulses each of α- and β-radiation were collected and used to determine the CCM short window. To discriminate α- and β-radiation, different radiation sources were tested. Test effectiveness can be directly calculated before fitting the distribution. The mean values μ' and standard deviations S of the P_{CCM}s of the samples can be directly calculated. Then, μ' were used to replace μ; and 2.355S was used to replace the FWHM. As such, Formula (3.2) was obtained and used to preliminarily estimate the discrimination effects of the CCM under different SSW (Size of the Short Window), as shown in figure 4 (note, the FoM' value is not the true FoM value):

$$\mathrm{FoM'} = \left|\left(\mu'_{\alpha} - \mu'_{\beta}\right) / \left(2.355 \cdot S_{\alpha} + 2.355 \cdot S_{\beta}\right)\right| \tag{3.2}$$

where μ' is the mean value of the discrimination parameter P_{CCM}s, S is the standard deviation of P_{CCM}s, and the right subscript indicates the corresponding radiation.

2020 JINST 15 P04008

The peak of the pulse served as the starting point of the short window, as shown in figure 1. As shown in figure 4(a), FoM' was maximized when the size of the short window was 4 for Detector A. As shown in figure 4(b), FoM' was maximized when the size of the short window was 186 for Detector B.

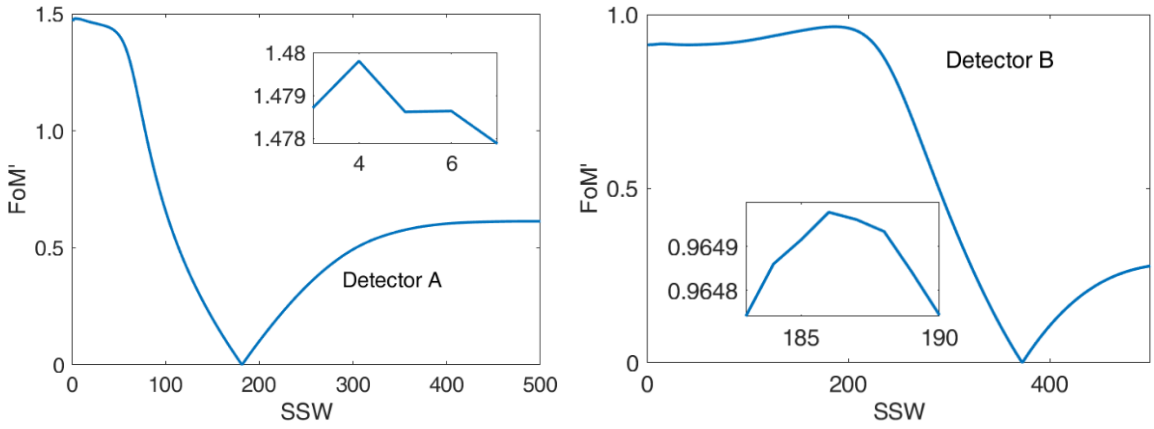

(a) (b)

Figure 4. FoM'with different discrimination parameters.

3.3 Processing with charge comparison method

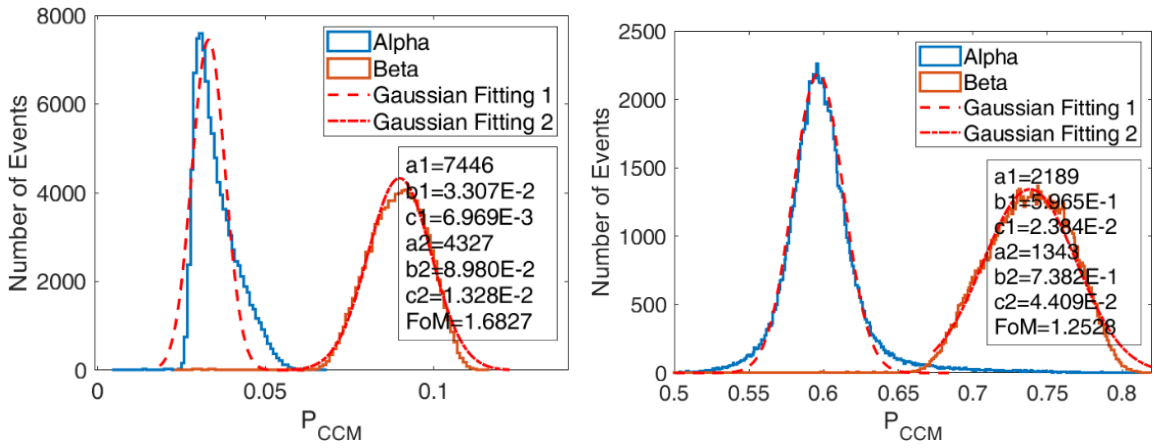

(a) (b)

Figure 5. Distribution after discrimination with the CCM.

One hundred thousand pulses each of α- and β-radiation were collected and used to test the effectiveness of the CCM discrimination. Discrimination parameter P_{CCM}s distributions are shown in figure 5. As shown in figure 5(a), the nuclear pulse shapes of α- and β-radiation from Detector A were clearly discriminated ($\mathrm{FoM}_{\mathrm{CCM,A}} = 1.6827$). In figure 5(b), no significant overlap was observed between the two distributions ($\mathrm{FoM}_{\mathrm{CCM,B}} = 1.2528$).

2020 JINST 15 P04008

3.4 Processing with time comparison method

The same 100,000 pulses each of α- and β-radiation were used to test the effectiveness of discriminating with the TCM. The distributions of the numbers of the rising-time points (corresponding with the rising times of the continuous voltage sequences) are shown in figure 6. As shown in figure 6(a), the nuclear pulse shapes of the α- and β-radiation from Detector A were discriminated ($\mathrm{FoM}_{\mathrm{TCM,A}} = 1.3796$). However, the nuclear pulse shapes of the α- and β-radiation from Detector B were not clearly discriminated with the TCM ($\mathrm{FoM}_{\mathrm{TCM,B}} = 0.6189$).

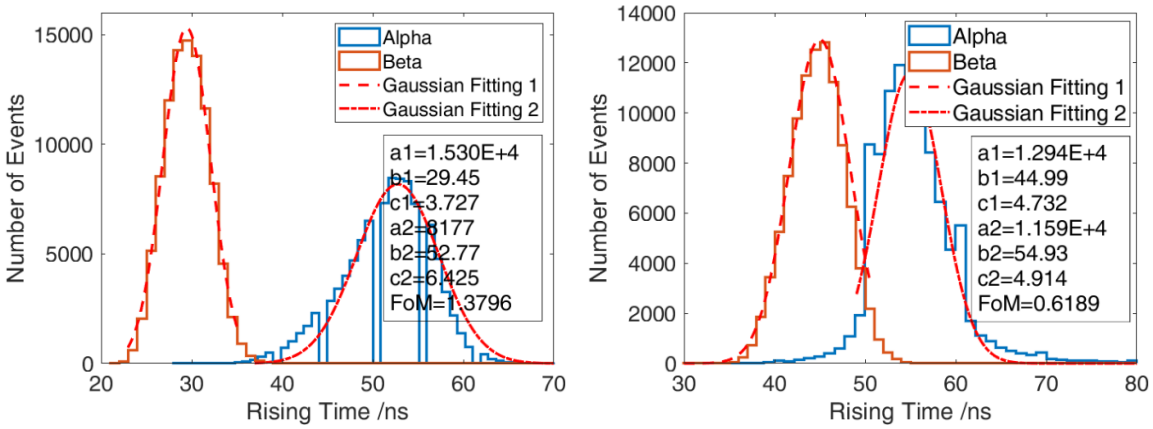

(a) (b)

Figure 6. Distribution after discrimination with the TCM.

4 Discussion and conclusion

In this work, two plastic scintillator detectors were used for the detection and discrimination of α- and β-radiation based on PSD. As shown in figure 5(a), α- and β-radiation can be clearly discriminated with the CCM. No significant overlap was observed between the two distributions (figure 5(b)); the CCM also worked well in discriminating pulses from Detector B. Compared with the CCM, the TCM did not perform as well. As shown in figure 6(b), the pulses from Detector B were not clearly discriminated. The CCM and Detector A performed better than the TCM and Detector B, respectively, because γ-radiation can be caught by the 1-cm-thick plastic scintillator.

In figure 7, the dashed lines show the numbers of α-radiation events m' misidentified as β-radiation. These values decreased when P_{CCM} thresholds increased. The dotted lines show the numbers of β-radiation events m' misidentified as α-radiation. These values increased when P_{CCM} thresholds increased. The total rate of misidentification δ (Delta) is defined in Formula (4.1) and represented as solid lines in figure 7 (the δ curves are concave, reaching minimums in middle intervals of P_{CCM}s):

$$\delta = \frac{m'_\alpha + m'_\beta}{m_\alpha + m_\beta} \times 100\% \tag{4.1}$$

where δ is the total rate of misidentification, m'_α is the number of β-radiation events misidentified as α-radiation, m'_β is the number of α-radiation events misidentified as β-radiation, m_α is the number of α-radiation events, and m_β is the number of β-radiation events.

2020 JINST 15 P04008

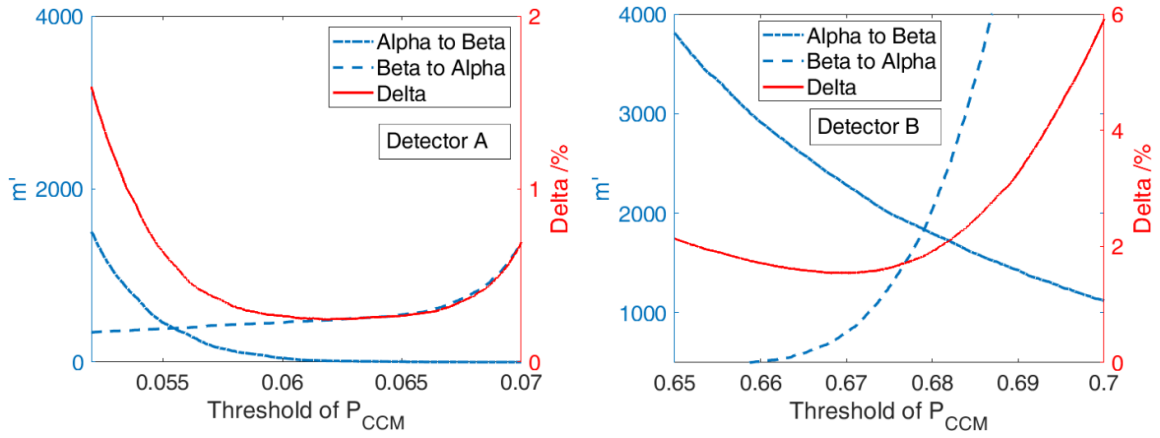

(a) (b)

Figure 7. Errors with different P_{CCM} thresholds.

The PSD effectiveness determines the discrimination parameters. For Detector A, δ was just under 0.25% when SSW was 4 and the P_{CCM} threshold was 0.06061 to 0.06189. For Detector B, δ was approximately 1.5% when SSW was 186 and the threshold was 0.6680 to 0.6711. Both detectors provided better discrimination than most current commercial detectors because commercial detectors typically have higher crosstalk between α- and β-radiation, i.e., if a detector errs in discriminating α-radiation as β-radiation, error is reduced by setting an appropriate PSD threshold. As the results from Detector B implied, the fluorescence yield of β-radiation events can be further improved to more efficiently detect low-energy β-radiation. This is a promising means to improving the effectiveness of detecting and discriminating between α- and β-radiation based on PSD.

Acknowledgments

This work was supported by the National Natural Science Foundation Joint Fund Key Project of China (U1865206) and the Research Learning and Innovative Experimental Plan for College Students of University of South China (2017XJXZ011).

References

[1] M. Nakhostin, *Digital discrimination of neutrons and γ-rays in liquid scintillation detectors by using low sampling frequency ADCs*, *Nucl. Instrum. Meth.* **A 916** (2019) 66.

[2] R.F. Langa et al., *Improved pulse shape discrimination in EJ-301 liquid scintillators*, *Nucl. Instrum. Meth.* **A 856** (2017) 26.

[3] A. Ivanova et al., *Fast neutron flux analyzer with real-time digital pulse shape discrimination*, *Nucl. Instrum. Meth.* **A 827** (2016) 13.

[4] E. Taqavi-Moqaddam, M. Safari and F.A. Davani, *Hybrid method for digital pulse shape discrimination in organic scintillation detectors*, 2019 *JINST* **14** P10004.

[5] C.-X. Zhang et al., *Discrimination of neutons and γ-rays in linquid scintlillator based on Elman neural network*, *Chin. Phys.* **C 40** (2016) 086204.

2020 JINST 15 P04008

[6] T. Yanagida, K. Watanabe, G. Okada and N. Kawaguchi, *Neutron and gamma-ray pulse shape discrimination of LiAlO2 and LiGaO2 crystals*, Nucl. Instrum. Meth. **A 919** (2019) 64.

[7] H. Bagán, A. Tarancón, G. Rauret and J. García, *Alpha/beta pulse shape discrimination in plastic scintillation using commercial scintillation detectors*, Anal. Chim. Acta **670** (2010) 11.

[8] I. Kreslo et al., *Pulse-shape discrimination of scintillation from alpha and beta particles with liquid scintillator and geiger-mode multipixel avalanche diodes*, 2011 *JINST* **6** P07009.

[9] C.-F. Yang, C.-Q. Feng, S.-B. Liu and Q. An, *FPGA-based α/γ pulse shape discrimination for BaF2 detector using 2-GSPS fast waveform sampling*, Nucl. Sci. Tech. **28** (2016) .

[10] C. Yang et al., *Alpha-gamma discrimination in BaF2 using FPGA-based feedforward neural network*, IEEE Trans. Nucl. Sci. **64** (2017) 1350.

[11] C. Zhenwei et al., *The Research on Matlab Simulation and Digital Pulse Shape Discrimination for Nuclear Signal*, *Chin. Nucl. Sci. Eng.* **36** (2016) 294.

[12] Y. Ling-fan et al., *Research of Nuclear Detector Circuit Fault Diagnosis Based on Support Vector Machine*, *Atomic Energy Sci. Technol.* **49** (2015) 1690.

[13] R. Winyard, J. Lutkin and G. McBeth, *Pulse shape discrimination in inorganic and organic scintillators. I*, Nucl. Instrum. Meth. **95** (1971) 141.

[14] J. Zhu, G. Gong, T. Xue, Z. Cao, L. Wei and J. Li, *Preliminary design of integrated digitizer base for photomultiplier tube*, IEEE Trans. Nucl. Sci. **66** (2019) 1130.

[15] Q. Wang et al., *Improvement on pulse-shape discrimination performance of SiPM array coupled* $Cs_2LiYCl_6{:}Ce^{3+}$ *detector*, 2019 *JINST* **14** P11005.

2020 JINST 15 P04008